A Performance Analysis of Alpha-Plane and Percentual Transmission Line Differential Protections

Igor Ferreira do Prado
State University of Santa Cruz
Ilhéus, BA, Brazil
Email:ifprado@uesc.br

Rodrigo Prado de Medeiros
Federal Rural University of the Semi-Arid
Caraúbas, RN, Brazil
Email:rodrigo.prado@ufersa.edu.br

Flávio Bezerra Costa
Federal University of Rio Grande do Norte
Natal, RN, Brazil
Email:flaviocosta@ect.ufrn.br

Kleber Melo e Silva
University of Brasília
Brasília, DF, Brazil
Email:klebermelo@unb.br

***Abstract*—This work accomplishes a comparative analysis between two transmission line differential protection methodologies available in commercial relays: percentage and alpha-plane differential protections. In order to verify the operation limits of the protections, several internal and external faults were simulated considering variations of the fault location, fault inception angle, fault impedance, and TC saturation. The alpha-plane method presented was the most accurate and fastest since the sequence units were not influenced by the fault impedance.**

***Index Terms*—Transmission Line Protection, Percentage Differential Protection, Alpha-Plane Differential Protection.**

I. INTRODUCTION

Transmission lines are important components of the power system since they connect the generation system to the distribution system. Therefore, the power system reliability is closely dependent of the transmission system. However, 70% of power system failures occurs on transmission lines [1] due to their length, which makes them more susceptible to weather conditions and vandalism. Therefore, a fast and reliable transmission line protection operation is required in order to prevent the emergence of faults, along all the power system, which would yield economic losses and major power delivery outages. [2].

The differential protection is a unitary protection, i.e., it protects the whole line, but it does not protect adjacent equipment or transmission lines. This protection presents several advantages over the distance protection, such as a better performance in transmission lines with serie compensation and no dependence of the voltage measurement in the most applications [3]. However, this technique demands a more complex communication system, which increases the implementation costs [4].

With the advent of new digital signal processing techniques and robust communication systems, the differential protection has become a promising alternative for the transmission line protection. Among the differential protection schemes applied in transmission lines, the most traditional one is the differential percentage [5]. However, the alpha-plane differential protection, which consists in a geometrical representation of the ratio of the current phasors that enter and leave a transmission line in a complex plane, has been commercially applied in the last years [6]. This technique was designed to present a more reliable operation when compared to the percentage one, since it provides, by means of a complex plan, information about the module and the phase of the local and remote currents.

This paper accomplishes a performance analysis between the transmission line percentage differential protection and alpha-plane differential protection, considering different challenging cases with variations of the fault type, fault location, fault inception angle, system loading, and fault impedance, in the presence and absence of current transformer (CT) saturation for internal and external faults. The performance of the alpha-plane protection method was slightly higher than the percentage differential protection.

II. TRANSMISSION LINE DIFFERENTIAL PROTECTION

The differential protection is based on the comparison of currents that flow to/from terminals of the protected element, providing reliable discrimination between internal and external faults. The limits of protection are defined by the connection of current transformers (CTs). In an internal fault condition, for instance, the differential relay sends the trip command for circuit breakers in order to isolate the equipment from the electrical system. The selectivity of this kind of protection is high, and internal faults can be well distinguished from external faults (faults outside the protection zone limits).

In transmission lines, CTs are usually too far apart. Therefore, a communication system with data synchronization is required to ensure the differential protection operates correctly with the current samples is a same time basis. The synchronization can be done by a communication channel as described in [7], or by the use of external time references, such as the Global Positioning System (GPS) [8]. In this work, phase (87LA, 87LB and 87LC), negative sequence (87LQ) and zero sequence (87LN) units were implemented.

Fig. 1 depicts all steps executed by the differential protection scheme, per sampling k. From the acquisition of the signal, performed by the CTs, until the tripping command, the following subroutines are executed: the preprocessing step, which consists in performing the digital acquisition of the CT currents using anti-aliasing filters and analog-to-digital converters, as described in [9]; the current phasor estimation, used to extract the module and angle of the fundamental component of local and remote currents; and the differential analysis, that implements logics of the percentage- and alpha-plane differential protections.

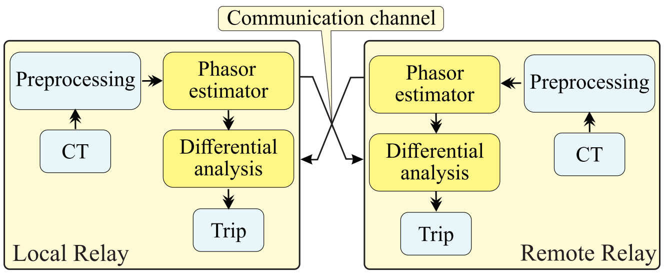

Figure 1. The differential relay block diagram.

A. Percentage Differential Protection Algorithm

Fig. 2 depicts the traditional configuration of a percentage differential protection circuit, composed by two CTs, two restriction coils (RC) and one operating coil (OC). In addition to the traditional operating coil, the restriction coil has been incorporated into the relay, which has the main function of reinforcing the actuation torque of the relay when an internal fault occurs and weakens it for external faults [10].

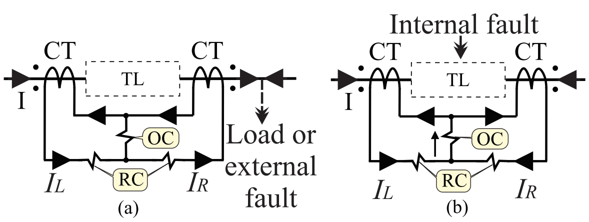

Figure 2. (a) Differential relay: (a) External fault; (b) Internal fault.

According to Fig. 2, in nominal loading or external fault situations, the current phasors ($\hat{I}_L$) and ($\hat{I}_R$) present the same magnitude and opposite directions, therefore no current flows in the operative coil, desensitizing the protection. Otherwise, for a fault occurring inside of the protection zone, there is a resulting current flux in the operative coil, which enables the protection operation. The operation and restriction currents (I_{op} and I_{res}) are given by [4]:

$$I_{op} = |\hat{I}_L + \hat{I}_R|, \tag{1}$$

$$I_{res} = \frac{|\hat{I}_L - \hat{I}_R|}{2}, \tag{2}$$

where $\hat{I}_L$ and $\hat{I}_R$ are currents at local and remote terminals, respectively. The protection operates when:

$$\begin{cases} I_{op} > SLP * I_{res}, \\ I_{op} > k_0, \end{cases} \tag{3}$$

where *SLP* defines the inclination of the differential characteristic curve; k_0 corresponds to a preset threshold (pickup current). In this application, k_0 is computed taking into account the capacitive current, that arises as a spurious differential current.

The differential characteristic curve is obtained from the solution of (3), with the definitions of the operating and restriction zones (Fig. 3).

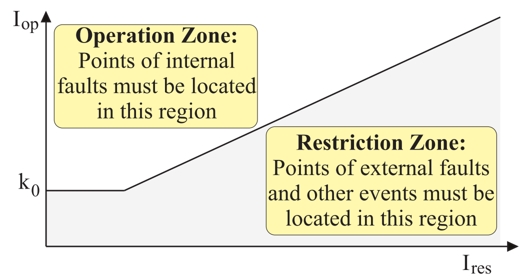

Figure 3. Characteristic percentage differential protection. [11]

B. Alpha-Plane Differential Protection Algorithm

The alpha-plane differential protection is based on the comparison of the ratio between the local relay current ($\hat{I}_L$) and the remote relay current ($\hat{I}_R$). Theses currents are usually obtained by the sum of the current phasor from all network elements (e.g. transmission lines, transformers) connected to the respective local and remote busbars wherein the protection act [12], [13]. Traditionally, is defined by the direct ratio of currents between the terminals, as follows

$$\hat{K} = \hat{I}_L / \hat{I}_R. \tag{4}$$

Fig. 4 depicts the alpha-plane differential characteristic, which consists in a circular region centered in the origin of the complex plane and delimits the border between the operation and restriction zones. When the value $\hat{K}$ exceeds the limits of the restriction zone and achieves the operation zone, a internal fault is detected.

According to Fig. 2, during an external fault or during nominal loading, $\hat{I}_L$ is approximately equal to $\hat{I}_R$, and due to the disposition of the CTs, they have opposite directions, therefore in this condition the point $\hat{K}$ in (4), in the complex plane, will be near to point (-1,0). The restriction area is characterized by the hatched area in Fig. 4. It is designed to accommodate the quotient $\hat{K}$ during normal operating conditions and external faults. During an internal fault condition, the value of $\hat{K}$ becomes positive for conventional faults in the protected zone, or negative, within circumference $R_2 = 1/R_1$, for outfeed faults The region called *"rainbow"* was choosed in this paper [3]. The operation and restriction zones were defined according to [14], taking into account the effects of the communication delays, capacitive currents and CT saturation.

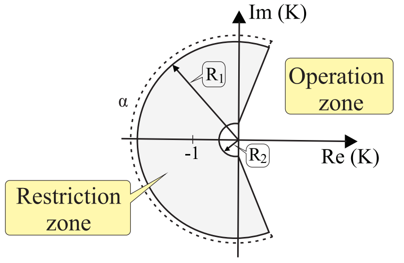

Figure 4. Differential element alpha plane protection.

III. Performance Evaluation

This section presents the results obtained from the comparative performance analysis of the percentage differential and alpha-plane algorithms for several simulated internal and external faults. Fig. 5 depicts a single line diagram of the 230 kV power system proposed by [15], which was modeled in the MATLAB/Simulink in this paper. The protection system was designed to protect a 200 km transmission line between bars 2 and 3. The transmission lines were modeled by considering its distributed parameters, and perfectly transposed.

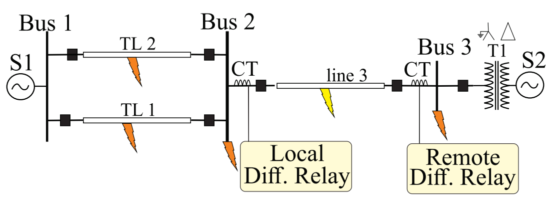

Figure 5. Power system model proposed by [15].

Two CTs described in [15] and configured at 800-5 A and 800-5 A taps were installed in the local and remote terminals, respectively. The currents were sampled at 15.36 kHz, and filtered through a second-order Butterworth anti-aliasing low-pass filter, with cutoff frequency of 960 Hz, for the elimination of the high-frequency content of the measured currents. After the analog filtering, the signals were subsampled to a rate of 960 Hz, which corresponds to 16 samplings per cycle of 60 Hz, and then the phasors were estimated based on the one-cycle Fourier algorithm.

The effect of the communication channel was considered taking into account a delay in the samples sent from each terminal in accordance with the communication protocol described in [16]. The time considered to emulate the message processing in the communication device is 3 ms, whereas the transmission of the signal through the optical fiber in 200 km takes 2 ms as described in [17]. Therefore, the total communication delay was 5 ms.

For the differential analysis, a relay was installed in each line terminal, with their respective three-phase, negative-sequence, and zero-sequence units.

Table I shows the fault parameters used to assess the differential protections, considering the presence and absence of CT saturation. All simulated cases were obtained by changing one parameter at time, the others were maintain at default values: fault inception angle of $\theta_f = 0°$, fault resistance of $r_f = 0$ Ω, and fault location at $d_f = 100$ km. Therefore, a thorough protection evaluation with challenging cases was performed.

Table I
Configuration for internal faults

Simulation variables	Values
Fault type	AG, AB, ABG, ABC
Fault location d_f(km)	20, 100, 180
Fault resistance $r_f(\Omega)$	0, 100, 300, 500, 600, 700, 900, 1000
Fault inception angle $\theta_f(°)$	0, 45, 90, 135, 180

Table II
Configuration for external faults

Simulation variables	Values
Fault type	AG, AB, ABG, ABC
Fault location d_f(km)	TL1, TL2, Bus 2, Bus 3
Fault resistance $r_f(\Omega)$	0, 100, 500
Fault inception angle $\theta_f(°)$	0, 45, 90

A. *External faults*

Fig. 6 depicts the performance of phase and sequence units considering single fault with and without CT saturation, out of protection zone on the local bar.

CTs are responsible for replicating currents to reduced values for system operation allowing correct and timely identification of faults and disturbances. During the saturation period, the CT secondary signals do not faithfully represent the current signals of the TL, i.e. the measures at the line terminals will be very different from each other, allowing the differential protection to act improperly.

The units of the percentage method have higher sensitivity to CT saturation for external faults, in Figs. 6(a), (c) and (e), the trajectory of the operation and restraint points is present for the entire fault period, in case of non-saturation the whole trajectory (black curve) remains in the restriction zone, while during saturation condition the measurement of the line currents are distorted, generating points outside the restriction zone, i.e. the trajectory presents points in the operating zone, featuring as an unsafe protection operation. After the saturation over, the measurements normalize leading the trajectory to the steady state point.

Regarding the alpha-plane method, the 87LA 87LG and 87LQ units does not show significant variation when CT saturation occurs only during the transient fault period. During external faults, even under saturation condition the current direction after CT continue in opposite directions, generating a negative ratio within the restriction zone.

During saturation, there is the possibility of improper actuation of differential protection for faults outside the protection zone, according Fig. 6, therefore an external fault detection routine based on the second harmonic current detection is used [18], which blocks the units from acting through an external saturation fault.

Performance for both methods was 100%, i.e. no external fault was detected as internal fault even in the presence of CT saturation.

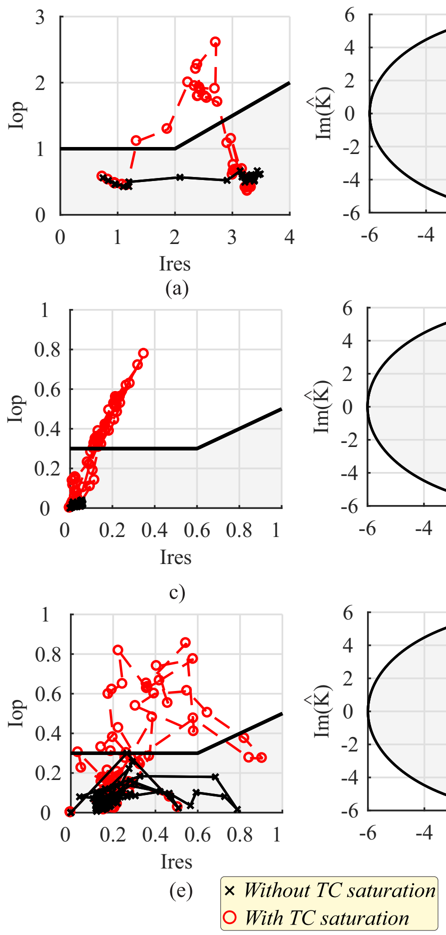

Figure 6. External fauts: (a) Percentage 87LA; (b) Alpha-plane 87LA; (c) Percentage 87LG; (d) Alpha-plane 87LG; (e) Percentage 87LQ; (f) Alpha-plane 87LQ.

B. Internal faults

1) Internal single-phase-to-ground fault: Fig. 7 depicts the performance of the phase, negative sequence and zero sequence units of the percentage and alpha-plane differential protections, for an internal single-phase fault considering different fault locations and resistances.

According to Figs. 7(a) and (b), the 87LA unit tends to lose sensitivity as the fault impedance increases for both methods. Taking the local terminal as reference, as fault distance and fault impedance increase, the sensitivity of the methods decreases until fault identification is no longer possible, leading the points associated to these situations to the restriction zone. The 87LA unit of the percentage method was able to detect 71.43%, whereas the same unit of the alpha-plane method was able to identify only 58.10% of the single-phase faults.

Regarding the 87LG (Figs. 7 (c) and (d)) and 87LQ units (Figs. 7 (e) and (f)), the alpha-plane method was immune to the fault impedance variation, being dependent only of the fault location. However, these units were still able to ensure, each one, a success rate of 100% for all single-phase faults. Or the other hand, the 87LG and 87LQ units of the percentage method were strongly affected by the fault impedance variation, failing to detect faults with resistances above of 900 Ω (success rate of 85,71%) for both units. Considering the general performance of the protections, the percentage method presented a success rate of 85,71% with an average delay time of 13.61 ms, whereas the alpha-plane method ensured a success rate of 100 % with an average delay time of 7.9 ms.

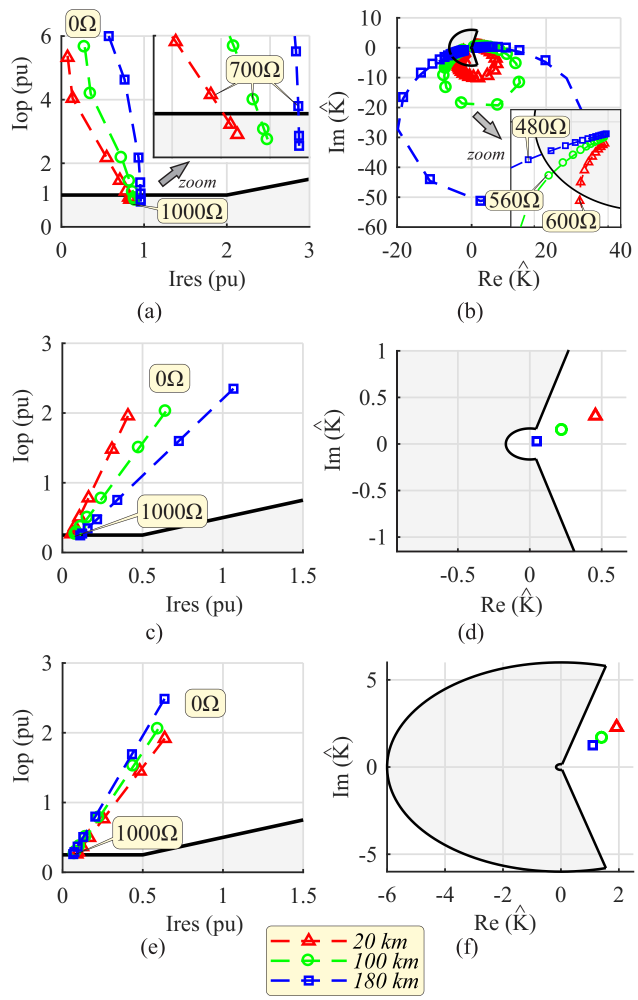

Figure 7. Internal single-phase-to-ground faults: (a) Percentage - 87LA unit; (b) Alpha-plane - 87LA unit; (c) Percentage - 87LG unit; (d) Alpha-plane - 87LG unit; (e) Percentage - 87LQ unit; (f) Alpha-plane - 87LQ unit.

2) Internal single-phase-to-ground fault with CT saturation: Fig. 8 compares the performance of protections under local CT saturation situation. A single phase fault was simulated with $d_f = 20$ km, $r_f = 600$ Ω, and $\theta = 0^o$. After CT saturation, the trajectory performed in the percentage and alpha-plane zones is affected causing a great time to reach the steady state. For example, in Fig. 8 (a) the 87LA unit for the percentage method detects the fault in 10 samples, while under saturation detection occurs in 13 samples, while the percentage method in fig. 8 (b) detects the fault in 5 and 9 samples for the case without and with saturation respectively. The same effect is presebt in the sequence units Figs. 8 (c), (d), (e) and (f).

The percentage of detection faults with saturation is is smaller than cases without saturation, in case of saturation faults with higher fault impedances, the methods do not operate properly.

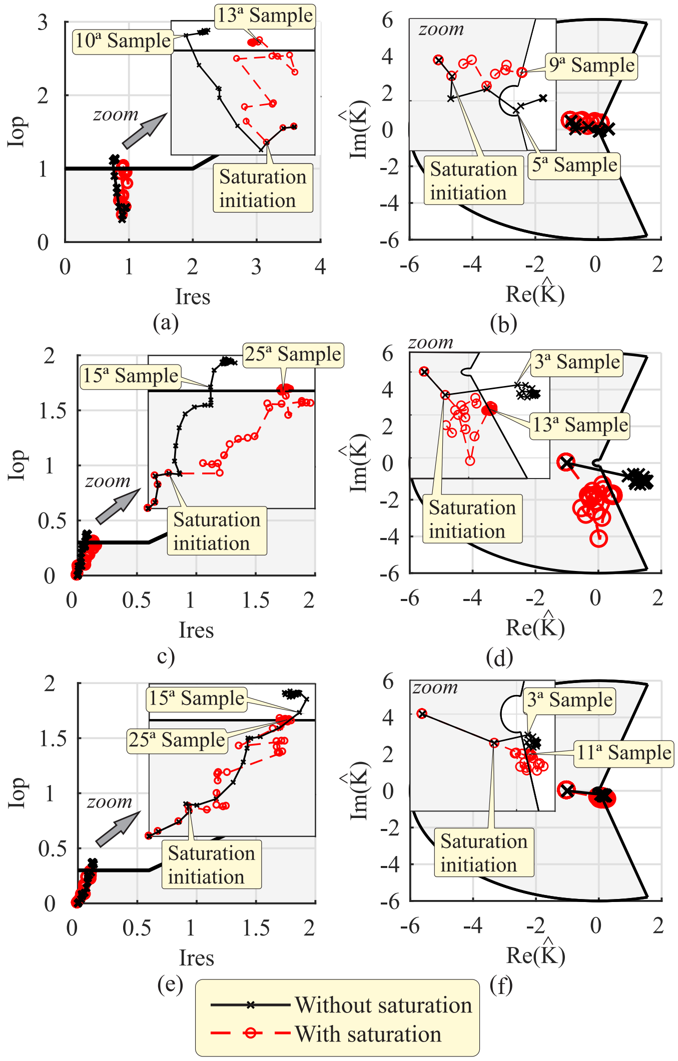

Figure 8. Internal single-phase-to-ground faults with CT saturation: (a) Percentage - 87LA unit; (b) Alpha-plane - 87LA unit; (c) Percentage - 87LG unit; (d) Alpha-plane - 87LG unit; (e) Percentage - 87LQ unit; (f) Alpha-plane - 87LQ unit.

3) Internal double-phase-to-ground fault - ABG: Fig. 9 depicts the performance of the protection units for internal double-phase-to-ground faults. According to Fig. 9(a), the performance of the 87LA unit of the percentage method was scarcely affected by the fault impedance variation and a success rate of 100% was achieved by this unit. Regarding the alpha-plane method, despite the 87LB unit present 99.3% of efficiency, the 87LA unit was able to detect all cases (100% of success rate) in Fig. 9(b).

Regarding the sequence units, the increase of the fault impedance affected the performance of the 87LG unit of the percentage method, which was not able to operate for faults with resistance above 600 Ω, ensuring a success rate of only 52.38%. The 87LQ unit operated for all faults (100% of success rate). For the alpha-plane method, the 87LG and 87LQ sequence units in Figs. 9(d) and (f) were not affected by the fault resistance in presenting success rates of 100%, each one.

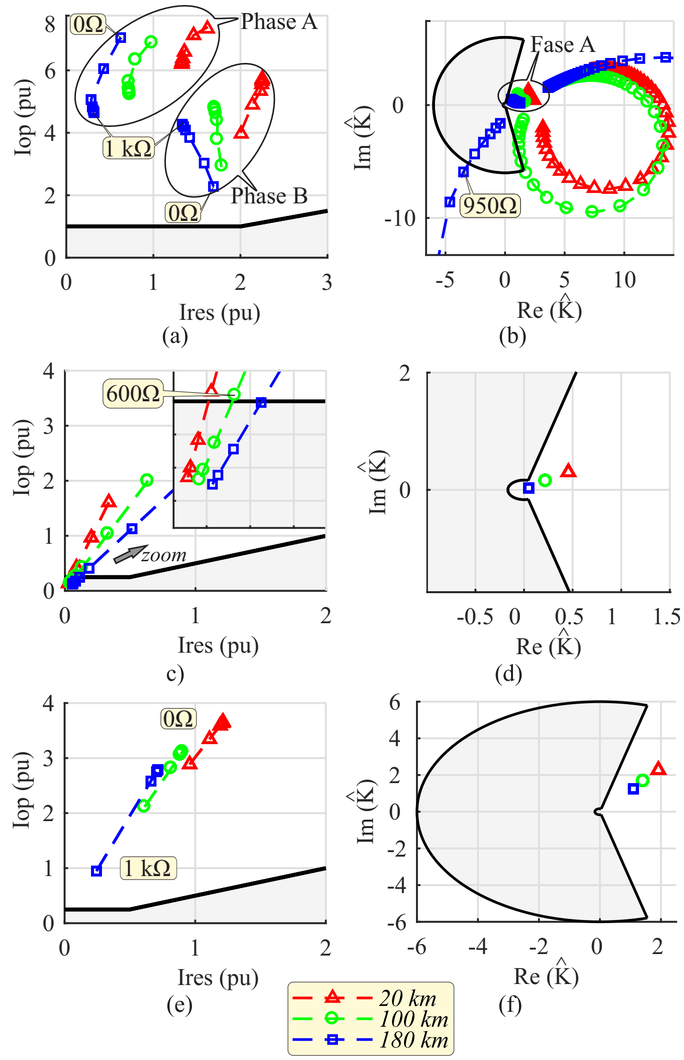

Figure 9. Internal double-phase-to-ground faults: (a) Percentage - 87LA unit; (b) Alpha-plane - 87LA unit; (c) Percentage - 87LG unit; (d) Alpha-plane - 87LG unit; (e) Percentage - 87LQ unit; (f) Alpha-plane - 87LQ unit.

4) Internal three-phase fault - ABC: Fig. 10 depicts the behavior of the phase units of both methods for an internal three-phase fault, considering $d_f = 100$ km, $r_f = 0\ \Omega$, and $\theta = 0^o$, with and without the presence of saturation.

Fig. 10 (a) and (b) show the behavior of the phase units 87LA, 87LB and 87LC of the percent method with and without local CT saturation, respectively. The trajectory of the operating and restraint points is represented from the pre-fault moment to the steady-state fault. The situation with CT saturation presents a greater variation in the trajectory behavior, however this aspect did not affect the detection for internal faults for the percentage method.

Considering the alpha-plane method in Fig. 10 (c) and (d), the CT saturation has influence on the phase units, analyzing the fault path for phase A during saturation there is a sample that is located in the restriction zone, causing the fault detection time to be extended for this unit. The steady-state for both cases is similar so that 100% of the faults were detected by all phases.

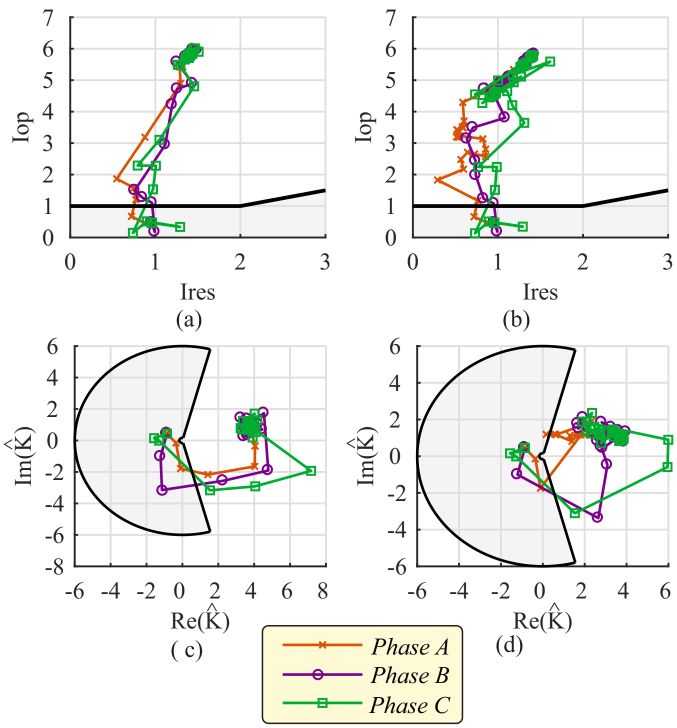

Figure 10. Internal three-phase faults: (a) Percentage - 87LA, 87LB and 87LC; (b) Alpha-plane - 87LA, 87LB and 87LC; (c) Percentage with saturation - 87LA, 87LB and 87LC, (d) Alpha-plane with saturation - 87LA, 87LB and 87LC

IV. Conclusion

This paper presented a comparison between the percentage and alpha-plane differential protection algorithms applied in the transmission line protection considering different internal and external fault scenarios, with variations of the fault type, fault location, fault resistance, fault inception angle, and system loading, as well as current transformer saturation. Both strategies presented a fast fault detection, with average detection time of 9.53 ms for the percentage and 7,77 ms for the alpha-plane method. The alpha-plane method presented the best performance, ensuring a success rate of 100 % against 98,43 % of the percentage one.

The internal faults not detected by the percentage method were of the high impedance single-phase type near the remote bar, however the alpha-plane method guarantees 100% detection of this type of fault due to the characteristic of the sequence units, since they are not influenced by the impedance of the fault. lack, whereas the conventional percentage method detected 95.3% of the single-phase faults.

The study performed in this work is important for the understanding of methodologies and aspects that affect the safety and reliability of a differential protection system for transmission lines, where the percentage differential protection presented limitations mainly in the identification of high impedance faults, whereas the alpha-plane method was the most robust and presented the fastest response time.

Acknowledgment

This work was supported by CAPES (Coordenação de Aperfeiçoamento de Pessoal de Nível Superior) and CNPq (Conselho Nacional de Desenvolvimento Científico e Tecnológico).

References

[1] Desligamentos forçados do sistema de transmissão. Agência Nacional de Energia Elétrica (ANEEL), 2017th ed, 2018.

[2] Y. G. Paithankar and S. Bhide, *Fundamentals of power system protection*. PHI Learning Pvt. Ltd., 2011.

[3] J. Roberts, D. Tziouvaras, G. Benmouyal, and H. Altuve, "The effect of multiprinciple line protection on dependability and security," in *proceedings of the 55th Annual Georgia Tech Protective Relaying Conference, Atlanta, GA*, 2001.

[4] G. Ziegler, *Numerical Differential Protection: Principles and Applications*. John Wiley & Sons, 2012.

[5] B. Kasztenny, G. Benmouyal, H. Altuve, and N. Fischer, "Tutorial on operating characteristics of microprocessor-based multiterminal line current differential relays," *Line Current Differential Protection: A Collection of Technical Papers Representing Modern Solutions*, 2014.

[6] Sel-411l: Advanced line differential protection, automation, and control system. Schweitzer Engineering Laboratories. [Online]. Available: https://selinc.com/products/411L/

[7] D. L. Mills, "Internet time synchronization: the network time protocol," *IEEE Transactions on Communications*, vol. 39, pp. 1482–1493, 1991.

[8] I. Hall, P. G. Beaumont, G. P. Baber, I. Shuto, M. Saga, K. Okuno, and H. Uo, "New line current differential relay using gps synchronization," in *2003 IEEE Bologna Power Tech Conference Proceedings,*, vol. 3, June 2003, p. 8pp.

[9] K. A. Tavares and K. M. Silva, "Evaluation of power transformer differential protection using the atp software," *IEEE Latin America Trans.*, vol. 12, no. 2, pp. 161–168, March 2014.

[10] E. C. Molas, K. M. Silva, and B. F. Kusel, "Teoria de comparadores aplicada na avaliação da atuação da proteção diferencial de linhas de transmissões no plano alfa," *XIX CBA Congresso Brasileiro de Automática*, 2012.

[11] R. P. Medeiros, F. B. Costa, , and M. A. D. Almeida, "Assessment of the main phasor-based power transformer differential protection elements," *SBSE - VI Simpósio Brasileiro de Sistemas Elétricos*, 2016.

[12] M. Hossain, I. Leevongwat, and P. Rastgoufard, "Revisions on alpha plane for enhanced sensitivity of line differential protection," *IEEE Transactions on Power Delivery*, pp. 1–1, 2018.

[13] R. G. Bainy and K. M. Silva, "Busbar differential protection based on generalized alpha plane," in *2017 Workshop on Communication Networks and Power Systems (WCNPS)*, Nov 2017, pp. 1–4.

[14] G. Benmouyal and T. Lee, "Sequence-current differential elements." *SEL Journal of Reliable Power*, 2004.

[15] P. S. Relaying and C. Committee. Emtp reference models for transmission line relay testing. IEEE. [Online]. Available: http://www.pes-psrc.org/kb/published/reports/EMTP%20Ref%20Model-Final.pdf

[16] D. Hou and D. Dolezilek, "Iec 61850 – what it can and cannot offer to traditional protection schemes," *SEL Journal of Reliable Power*, vol. 1, no. 2, pp. 1–11, 2010.

[17] F. B. Costa, A. Monti, F. V. Lopes, K. M. Silva, P. Jamborsalamati, and A. Sadu, "Two-terminal traveling-wave-based transmission-line protection," *IEEE Transactions on Power Delivery*, vol. 32, no. 3, pp. 1382–1393, June 2017.

[18] IEEE, "Guide for protective relay applications to power transformers." *IEEE STANDARDS ASSOCIATION. C37.91-2000.*